



Fractional electro-magneto transport of blood modeled with magnetic particles in cylindrical tube without singular kernel

S. Uddin¹ · M. Mohamad¹ · Mohammad Rahimi-Gorji² · R. Roslan¹ · Ibrahim M. Alarifi³

Received: 10 April 2019 / Accepted: 16 May 2019 / Published online: 24 May 2019
© Springer-Verlag GmbH Germany, part of Springer Nature 2019

Abstract

The electro-kinetic transport of blood flow mixed with magnetic particles in the circular channel was investigated. The flow was subjected to an external electric and uniform magnetic field. The fluid was driven by pressure gradient and perpendicular magnetic field to the flow direction. Due to the usefulness and suitability of Caputo–Fabrizio fractional order derivative without singular kernel in fluid flow modeling and mass transfer phenomena, the governing equations were modeled as Caputo–Fabrizio time fractional partial differential equations and solved for $\alpha \in (0, 1]$. The analytical solutions for the velocities of blood flow and magnetic particles were obtained by using Laplace, finite Hankel transforms and Robotnov and Hartley’s functions, respectively. Mathematica software was used to simulate the influences of fractional parameter α , Hartmann number and Reynolds number on the velocities of blood and magnetic particles. The findings are important for controlling bio-liquids in the devices used for analysis and diagnosis in biological and medical applications.

1 Introduction

One of the alternate ways of delivering blood flow is electro-magneto flow driven by externally applied electric and magnetic fields. It involves both magnetic and electrostatic collisions between the magnetically charged particles in the ionized solution. Considerable amount of work have been done to identify various blood flow patterns and characteristics in the presence of magnetic field and electric current. Electro-magneto blood flow has been implemented in surgical treatments and cancer (tumor) operations.

The artificial blood velocity was measured experimentally at different magnetic fields strength and it was noticed that the velocities of blood and magnetic particles velocity fell tremendously in the presence of magnetic field (Sharma et al. 2015). Although the behaviors of magnetic particles and blood are quiet similar, the magnetic particles velocity is lower than blood velocity due to the drag force and other resistive forces (Shah et al. 2016a). In micro channels the heat conversion capacity and fluid flow can be regulated in the non-local system (Roslan et al. 2016) as it flow faster. Moreover the channel temperature can be adjusted via manipulating the Joule’s parameter. The temperature profile reported was different as compared to those reported by using other model. There was greater heat transfer rate for the oscillatory movement of the triangular wave form of the temperature profile.

Rubbab et al. (2017) obtained the microscopic results such as the typical material length scale, which is important for one to perceive the fluid characteristics. Moreover, all the classical fluid results can be recovered by setting the typical length scale to zero in the couple-stress fluid. Kumar et al. (2012) found that the blood velocity would increase upon applying the body acceleration and combining the body acceleration with magnetic field. Their study is helpful for treating cardiovascular, blood borne and hypertension diseases. The study conducted by Singh and Rathee (2011) was limited to certain magnetic field

✉ Ibrahim M. Alarifi
i.alarifi@mu.edu.sa

Mohammad Rahimi-Gorji
mohammad.rahimigorji@ugent.be; m69.rahimi@yahoo.com

R. Roslan
rozaini@uthm.edu.my

¹ Department of Mathematics and Statistics, Faculty of Applied Sciences and Technology, Universiti Tun Hussein Onn Malaysia, Pagoh, 84600 Muar, Johor, Malaysia

² Faculty of Medicine and Health Science, Ghent University, 9000 Gent, Belgium

³ Department of Mechanical and Industrial Engineering, College of Engineering, Majmaah University, Majmaah 11952, Saudi Arabia

range. They studied the blood flow in hypertensive patients and in arteries having blockages. Also, there are some references which performed in this field (Alsagri et al. 2019; Gul et al. 2019; Ahmad 2019; Souayeh et al. 2016, 2017a, b, 2019; Raju et al. 2019; Ahmad and Khan 2019; Krishna et al. 2019; Ahmed et al. 2018; Hussanan et al. 2019; Bezi et al. 2018; Alarifi et al. 2018, 2019).

Obstructions in water and sewage system pipelines are major concerns nowadays. Patel et al. (2012) modeled the constriction by using sinusoidal model. The axial velocity was then solved using the simple pipeline network model. Santapuri (2016) indicates the practicality and usefulness of his framework through multi-ferrous material of the symmetric hexagonal crystal in which the limitations on the material constants were also specified. Buchukuri et al. (2016) investigated the oscillating singularities by using the potential method and the pseudo-differential equations on 35 manifolds with boundary. The uniqueness and existence of the solutions were then established. Bhatti et al. (2017) have performed both numerical and experimental works on MHD and heat transfer of non-Newtonian flows. By using the nano fluid model, Sher et al. (2017) focused on different types of nano-particles which were platelet, cylinder and brick shape in the study of unsteady, non-uniform and peristaltic flow. The thermal conductivity, temperature and axial velocity profiles of these nano-particles were sequenced as bricks < cylinder < platelets. The size of trapped bolus was the largest for bricks as compared to platelets in the nano-fluid model. Usman et al. (2018) found that the heat transfer and fluid flow results for two-phase, unsteady magnetized flow with nano-particles obtained using the fourth order Runge–Kutta and scheme the differential transform method were quiet similar.

Tripathi et al. (2018) noticed that the axial velocity in the core region was increased the electric field whereas the opposite behavior was observed at micro-channel walls. On the other hand, there was a reduction in the number of trapped boluses. In the model proposed by El-Borhany (2017), flow parameters affecting the convergence of the numerical solution in the regularization process were reported. At large ratio $\frac{\xi}{\tau}$, bifurcated solutions and secondary vortices were more apparent. Falade et al. (2017) found that by raising the injection/suction parameter affected by thin thermal radiation optics in the Oscillatory MHD flow through permeable medium, parameter such as the flow velocity, fluid temperature and skin friction were elevated thus reducing the heat transfer rate on the heated plate. Heat transfer of MHD couple stress fluid flow had major contributions in maximizing heat transfer and reducing skin frictions (Shah et al. 2016b). Moreover by

enhancing parameter such as Hartmann number, porosity, heat source and couple stress parameter of the flow, the heat transfer rate could be enhanced significantly meanwhile, if high heat sink parameter and Prandtl number were employed the heat transfer rate would decrease.

Sharma and Sharma (2014) investigated the effect of relaxation time on both spatial and temporal temperature profiles. The effects of several parameters on the temperature fluctuations were graphically analyzed. Tanveer (2016) solved the velocity distribution model in coronary arteries subjected to external magnetic field and fatty particles. The performed study was 65 is helpful in the treatment of various cardiovascular and arterial diseases. Caputo and Fabrizio (NFDt) (2015) modified the old Caputo fractional order derivative (UFDt) so that is free from singular kernel. In NFDt, fractional order works on both temporal and spatial variable. Temporal variable is more suitable for Laplace transform. While, the spatial variables is more suitable for Fourier transform. Time fractional order derivative model gives a non-local system which is free from the singular kernel, which is able to explain the multifariousness of the medium and the oscillation at different levels, which are not well defined in the classical local system or in the fractional order system with singular kernel. For NFDt at $\alpha = 1$, the classical local system is recovered. Recently, Morales-Delgado et al. (2019) studied the dynamics of the oxygen diffusion through capillary to tissues using Caputo–Fabrizio and Liouville–Caputo fractional derivatives by using Laplace homotopy method.

The purpose of this paper is to deal with application of Caputo–Fabrizio fractional derivative to solve unsteady viscous flow of blood filled with magnetic particles subject to an oscillating pressure gradient through a cylindrical tube. The flow acted upon by external electric field and magnetic field normal to the flow direction.

2 Mathematical model

Consider three-dimensional unsteady viscous flow of blood mixed with magnetic particles (iron rich particles) under the action of an oscillating pressure gradient inside the circular cylinder of radius R_0 . The transport of the blood and magnetic particles in the channel is exposed to the external electric field \vec{E} and magnetic field \vec{B} as shown in Fig. 1. The effect of electromagnetic on the velocity profiles of blood flow and magnetic particles flow has been focused in depth.

Governing continuity and momentum equations for the electro-magnetic transport of blood mixed with magnetic

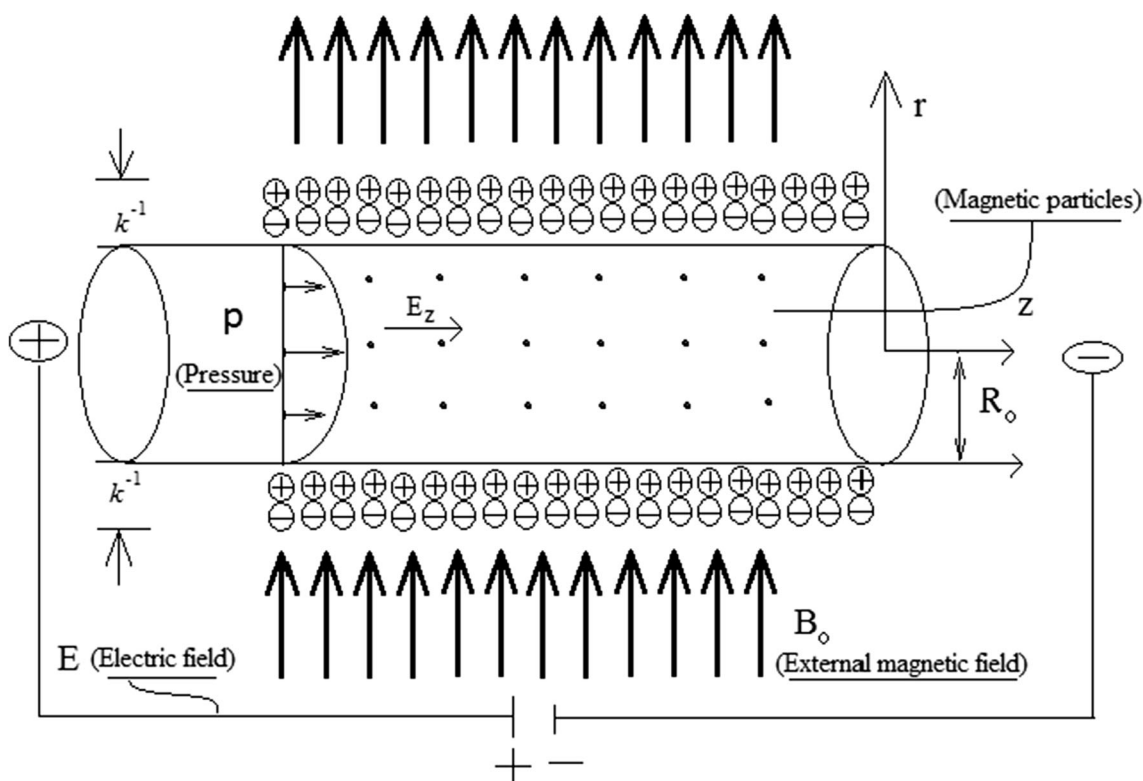


Fig. 1 Electro-magneto blood flow transport model

particles in the cylindrical coordinates (r, θ, z) is given by (Shah et al. 2016a):

$$\frac{\partial u_r}{\partial r} + \frac{u_r}{r} + \frac{\partial u_z}{\partial z} = 0 \tag{1}$$

$$\begin{aligned} &\rho \left(\frac{\partial u_r}{\partial t} + u_r \frac{\partial u_r}{\partial r} + \frac{u_\theta}{r} \frac{\partial u_r}{\partial \theta} - \frac{u_\theta^2}{r} + u_z \frac{\partial u_r}{\partial z} \right) \\ &= -\frac{\partial p}{\partial r} + \rho f_r + \mu \left[\frac{\partial}{\partial r} \left(\frac{1}{r} \frac{\partial (ru_r)}{\partial r} \right) + \frac{1}{r^2} \frac{\partial^2 u_r}{\partial \theta^2} - \frac{2}{r^2} \frac{\partial u_\theta}{\partial \theta} + \frac{\partial^2 u_r}{\partial z^2} \right] \end{aligned} \tag{2}$$

$$\begin{aligned} &\rho \left(\frac{\partial u_\theta}{\partial t} + u_r \frac{\partial u_\theta}{\partial r} + \frac{u_\theta}{r} \frac{\partial u_\theta}{\partial \theta} + \frac{u_r u_\theta}{r} + u_z \frac{\partial u_\theta}{\partial z} \right) \\ &= -\frac{1}{r} \frac{\partial p}{\partial r} + \rho f_\theta + \mu \left[\frac{\partial}{\partial r} \left(\frac{1}{r} \frac{\partial (ru_\theta)}{\partial r} \right) + \frac{1}{r^2} \frac{\partial^2 u_\theta}{\partial \theta^2} + \frac{2}{r^2} \frac{\partial u_r}{\partial \theta} + \frac{\partial^2 u_\theta}{\partial z^2} \right] \end{aligned} \tag{3}$$

$$\begin{aligned} &\rho \left(\frac{\partial u_z}{\partial t} + u_r \frac{\partial u_z}{\partial r} + \frac{u_\theta}{r} \frac{\partial u_z}{\partial \theta} + u_z \frac{\partial u_z}{\partial z} \right) \\ &= -\frac{\partial p}{\partial r} + \rho f_z + \mu \left[\frac{1}{r} \frac{\partial}{\partial r} \left(r \frac{\partial u_z}{\partial r} \right) + \frac{1}{r^2} \frac{\partial^2 u_z}{\partial \theta^2} + \frac{\partial^2 u_z}{\partial z^2} \right]. \end{aligned} \tag{4}$$

For the governing continuity and Navier–Stokes equations of the blood flow model in the cylindrical coordinates, we are assuming the following realistic assumptions.

1. Only one velocity component is non-zero i.e.; $u_z = u$ at z -direction. Thus $u_r = 0 = u_\theta$
2. Axial component of the velocity is independent of the angular location, hence $\frac{u_\theta}{\partial \theta} = 0$.

The above governing equations from Eqs. (1)–(4) are then reduce to

$$\frac{\partial u_z}{\partial z} = 0 \tag{5}$$

$$\rho \left(\frac{\partial u_z}{\partial z} \right) = -\frac{\partial p}{\partial z} + \eta \frac{\partial}{\partial r} \left(\frac{1}{r} \frac{\partial (ru_z)}{\partial r} \right) + F_{em} + F_{uv}. \tag{6}$$

2.1 Electro-magnetic field and relative forces

The electro-magnetic field force F_{em} and the force F_{uv} due to the motion between blood and magnetic particles can be represented as

$$\begin{aligned} F_{em} &= J \times B = \sigma(E + V \times B) \times B \\ &= -\sigma^2 B^2 u(r, t) \vec{j} - \rho_e E \\ &= -\sigma^2 B^2 u(r, t) \vec{j} - \rho_e E_z k \end{aligned} \tag{7}$$

$$F_{uv} = K_m N \{v(r, t) - u(r, t)\} \tag{8}$$

where B_0 and E_z are the magnetic and electric field in axial direction. J is the density of current, \vec{j} is the unit vector in z -direction, $u_z = u(r, t) \vec{j}$ is the blood flow velocity

component and $v(r, t)$ is the magnetic particles velocity component in z-direction. $\rho_e = -\varepsilon \kappa^2 \psi(r)$ is the net charge density. In $\kappa^2 = \frac{2z_0^2 e_0^2 n_0}{\varepsilon k_B T_a}$, ε is the dielectric constant, κ is the Debye–Hukel parameter, κ^{-1} is the thickness of electrical double layer, n_0 is the ionic concentration in the bulk phase, e_0 is the electronic charge, k_B is the Boltzmann constant, T_a is the absolute temperature. K_m is the stokes constant, N is the number of magnetic particles per unit volume.

2.2 Bio-fluid velocity model

The governing momentum in Eq. (6) is representing the unsteady, axisymmetric transport of the blood flow model in the presence of external pressure gradient and electro-magnetic field:

$$\frac{\partial u(r, t)}{\partial t} = \frac{1}{\rho} (A_0 + A_1 \cos(\omega t)) + v \left(\frac{\partial^2 u(r, t)}{\partial r^2} + \frac{1}{r} \frac{\partial u(r, t)}{\partial r} \right) + \frac{K_m N \{v(r, t) - u(r, t)\}}{\rho} - \frac{\sigma^2 B^2 u(r, t)}{\rho} + \frac{\varepsilon \kappa^2 \psi(r) E_z}{\rho}, A_0 > 0 \quad (9)$$

where A_0 and A_1 are the pulsatile components of the pressure gradient giving rise to the systolic and diastolic pressure. Newton's second law of motion governs the movement of magnetic particles in the blood flow

$$m \frac{\partial v(r, t)}{\partial t} = K_m \{u(r, t) - v(r, t)\} \quad (10)$$

where $u(r, t)$ and $v(r, t)$ are the blood flow and magnetic particles velocity in the axial direction respectively and m is the magnetic particles average mass, ρ is the fluid density and v is the kinetic viscosity.

Caputo–Fabrizio time fractional order model of Eqs. (9) and (10) is obtained by taking t and multiplying both sides of the equations by $\frac{\partial}{\partial t} = D_t^{(\alpha)}$, which has the dimension of t

$$\lambda^\alpha D_t^{(\alpha)} u(r, t) = \frac{\lambda}{\rho} (A_0 + A_1 \cos(\omega t)) + \lambda v \left(\frac{\partial^2 u(r, t)}{\partial r^2} + \frac{1}{r} \frac{\partial u(r, t)}{\partial r} \right) + \frac{K_m N \lambda}{\rho} \{v(r, t) - u(r, t)\} - \frac{\sigma^2 B_0^2 u(r, t) \lambda}{\rho} + \frac{\varepsilon \kappa^2 E_z \psi(r) \lambda}{\rho}, A_0 > 0 \quad (11)$$

and

$$\lambda^\alpha D_t^{(\alpha)} v(r, t) = \frac{K_m \lambda}{m} \{u(r, t) - v(r, t)\}. \quad (12)$$

The initial and boundary conditions of the blood flow inside circular cylinder of radius R_0 are

$$\begin{aligned} u(r, 0) = 0, v(r, 0) = 0, r \in [0, R_0] \\ u(R_0, t) = 0, v(R_0, t) = 0, t > 0. \end{aligned} \quad (13)$$

To study the non-dimensional model introducing the non-dimensional variables

$$\begin{aligned} r' = \frac{r}{R_0}, \quad t' = \frac{t}{\lambda}, \quad u' = \frac{u}{u_0}, \quad v' = \frac{v}{v_0}, \quad \omega = \lambda \omega, \\ A'_0 = \frac{\lambda A_0}{\rho u_0}, \quad A'_1 = \frac{\lambda A_1}{\rho u_0}, \quad \psi' = \frac{\psi}{\psi_0} \end{aligned} \quad (14)$$

where u_0 is the characteristic velocity. Equations (11)–(13) becomes (after dropping dashes)

$$\begin{aligned} D_t^{(\alpha)} u(r, t) = A_0 + A_1 \cos(\omega t) + \frac{1}{\text{Re}} \left(\frac{\partial^2 u(r, t)}{\partial r^2} + \frac{1}{r} \frac{\partial u(r, t)}{\partial r} \right) \\ + R \{v(r, t) - u(r, t)\} - Ha^2 u(r, t) \\ + K^2 \psi(r), A_0 > 0 \end{aligned} \quad (15)$$

$$G \cdot D_t^{(\alpha)} v(r, t) = u(r, t) - v(r, t) \quad (16)$$

$$\begin{aligned} u(r, 0) = 0, v(r, 0) = 0, r \in [0, 1] \\ u(1, t) = 0, v(1, t) = 0, t > 0 \end{aligned} \quad (17)$$

where $K^2 = \frac{\varepsilon \kappa^2 E_z \lambda}{\rho}$ is the electro-kinetic width, $Ha^2 = \frac{\sigma^2 B_0^2 \lambda}{\rho}$ is the Hartmann number, $\text{Re} = \frac{R_0^2}{\lambda \rho}$ is the Reynolds number, $R = \frac{K_m N \lambda}{\rho}$ is the particles concentration parameter and $G = \frac{m}{K_m \lambda}$ is the mass parameter of magnetic particles.

2.3 A new definition of fractional derivative without singular kernel NFDt

In 1967 Caputo define fractional time derivative with singular kernel usually denoted as UFD_t,

$$D_t^{(\alpha)} f(t) = \frac{1}{\Gamma(1-\alpha)} \int_a^t \frac{\dot{f}(\tau)}{(t-\tau)^\alpha} d\tau, \quad (18)$$

with $\alpha \in [0, 1]$ and $a \in [-\infty, t)$, $f \in H^1(a, b)$, $b > a$ where H^1 is the class of all integrable functions on $[a, b]$. In Eq. (18) kernel has a singular value at $t = \tau$. This was further modified by Caputo and Fabrizio (2015) and called as NFDt, by removing the singularity from the definition:

$$D_t^{(\alpha)} f(t) = \frac{M(\alpha)}{(1-\alpha)} \int_a^t \dot{f}(\tau) \exp\left(-\frac{\alpha(t-\tau)}{1-\alpha}\right) d\tau, \quad (19)$$

where $M(0) = M(1) = 1$ (condition of the function normalization). In addition to the absence of singularity in the new definition of fractional derivative $NFDt$, it has another property that it coincides with the old definition $UFDt$ at zero for a constant $f(t)$. Moreover $f(t) \notin H^1(a, b)$ can also be operated by $NFDt$. The equivalent form of the definition in Eq. (19) assumes the form

$$\tilde{D}_t^{(\sigma)} f(t) = \frac{N(\sigma)}{\sigma} \int_a^t \dot{f}(\tau) \exp\left(-\frac{(t-\tau)}{\sigma}\right) d\tau. \tag{20}$$

One of the property of $NFDt$ is related to the computation of Laplace transform (LT) with variable s , by taking $a = 0$ in the definition in Eq. (20)

$$LT [D_t^{(\alpha)}]f(t) = \frac{sLT [f(t)] - f(0)}{s + \alpha(1 - s)}. \tag{21}$$

2.4 Solution to the problem

Laplace transform is most suitable in case of temporal variable t in the blood flow model discussed in Eqs. (15) and (16) and boundary condition in (17). After transformation we have

$$\begin{aligned} \frac{s\bar{u}(r, s)}{s + \alpha(1 - s)} &= \frac{1}{s} (A_0 + K^2\psi(r)) + \frac{1}{\text{Re}} \left(\frac{\partial^2 \bar{u}(r, s)}{\partial r^2} + \frac{1}{r} \frac{\partial \bar{u}(r, s)}{\partial r} \right) \\ &+ R\{\bar{v}(r, t) - \bar{u}(r, t)\} - Ha^2 \bar{u}(r, t) \\ &+ \frac{A_1 s}{s_2 + \omega^2}, A_0 > 0 \end{aligned} \tag{22}$$

$$G \cdot \frac{s\bar{v}(r, s)}{s + \alpha(1 - s)} = \bar{u}(r, s) - \bar{v}(r, s) \tag{23}$$

$$\bar{u}(1, s) = 0, \bar{v}(1, s) = 0. \tag{24}$$

Substituting $\bar{v}(r, s)$ from Eq. (23) into Eq. (23) and then taking finite Hankel transform with respect to the radial coordinate r along with the boundary condition in Eq. (24),

$$\begin{aligned} \bar{u}_H(\varsigma_n, s) &\left(\frac{s}{s + \alpha(1 - s)} - R \frac{s + \alpha(1 - s)}{s + sG + \alpha(1 - s)} + Ha^2 + R + \frac{\varsigma_n^2}{\text{Re}} \right) \\ &= \left(\frac{1}{s} A_0 + \frac{A_1 s}{s^2 + \omega^2} \right) \frac{J_1(\varsigma_n)}{\varsigma_n} + \frac{1}{s} K^2 \frac{\varsigma_n}{\varsigma_n^2 + K^2} J_1(\varsigma_n) \end{aligned} \tag{25}$$

where $\bar{u}_H(\varsigma_n, s) = \int_0^1 r u(r, s) J_0(\varsigma_n, s) dr$ is representing the finite Hankel transform of the velocity function $\bar{u}(r, s) = LT [u(r, t)]$ and $\varsigma_n, n = 1, 2, \dots$ are the positive roots of the equation $J_0(x)=0$, here J_0 is the Bessel function of order zero and belong to the first kind. By simplifying the coefficient of $\bar{u}_H(\varsigma_n, s)$ in Eq. (25), we have

$$\begin{aligned} \bar{u}_H(\varsigma_n, s) &= \frac{s^2 m_{2n} + s m_{3n} + m_{4n}}{s^2 m_{5n} + s m_{6n} + \alpha^2} \\ &\times \left\{ \left(\frac{1}{s} A_0 + \frac{A_1 s}{s^2 + \omega^2} \right) \frac{J_1(\varsigma_n)}{\varsigma_n} + \frac{1}{s} K^2 \frac{\varsigma_n}{\varsigma_n^2 + K^2} J_1(\varsigma_n) \right\} \end{aligned} \tag{26}$$

$$\begin{aligned} \bar{u}_H(\varsigma_n, s) &= \left\{ \frac{m_{9n}}{s - m_{7n}} + \frac{m_{10n}}{s - m_{8n}} \right\} \\ &\times \left\{ \left(\frac{A_0}{s} + \frac{A_1 s}{s^2 + \omega^2} \right) \frac{J_1(\varsigma_n)}{\varsigma_n} + \frac{K^2}{s} \frac{\varsigma_n}{\varsigma_n^2 + K^2} J_1(\varsigma_n) \right\} \end{aligned} \tag{27}$$

where the parameters introduced in Eqs. (26) and (27) for simplifying the coefficient of $\bar{u}_H(\varsigma_n, s)$ in Eq. (25) are as follows

$$\begin{aligned} m_{1n} &= Ha^2 + R + \frac{\varsigma_n}{\text{Re}}, \\ m_{2n} &= 1 + G - \alpha - R - R\alpha^2 + 2R\alpha + m_{1n} \\ &+ \alpha^2 m_{1n} - 2\alpha m_{1n} + Gm_{1n} - G\alpha m_{1n}, \\ m_{3n} &= \alpha + 2R\alpha^2 - 2R\alpha - 2m_{1n}\alpha^2 + 2\alpha m_{1n} + G\alpha m_{1n}, \\ m_{4n} &= \alpha^2 m_{1n} - R\alpha^2, \\ m_{5n} &= 1 + \alpha^2 - 2\alpha + G - G\alpha, \quad m_{6n} = -2\alpha^2 + 2\alpha + G\alpha, \\ m_{7n} &= \frac{-m_{3n} + \sqrt{m_{3n}^2 - 4m_{2n}m_{4n}}}{2m_{2n}}, \\ m_{8n} &= \frac{-m_{3n} - \sqrt{m_{3n}^2 - 4m_{2n}m_{4n}}}{2m_{2n}}, \quad m_{9n} = \frac{m_{7n}^2 m_{5n} + m_{7n} m_{6n} + \alpha^2}{m_{7n} - m_{8n}}, \\ m_{10n} &= \frac{m_{8n}^2 m_{5n} + m_{8n} m_{6n} + \alpha^2}{m_{8n} - m_{7n}}. \end{aligned} \tag{28}$$

Laplace transform of the image function $\bar{u}_H(\varsigma_n, s)$ discussed in Eq. (27) is obtained by using the Robotnov and Hartley’s functions

$$LT^{-1} \left[\frac{1}{s^a + b} \right] = F_a(-b, t) = \sum_{n=0}^{\infty} \frac{(-b)^n t^{(n+1)a-1}}{\Gamma((n+1)a)}, a > 0 \tag{29}$$

$$\begin{aligned} LT^{-1} \left[\frac{s^c}{s^a + b} \right] &= R_{a,c}(-b, t) \\ &= \sum_{n=0}^{\infty} \frac{(-b)^n t^{(n+1)a-1-c}}{\Gamma((n+1)a - c)}, \text{Real}(a - c) > 0 \end{aligned} \tag{30}$$

$$\begin{aligned} u_H(\varsigma_n, t) &= \frac{J_1}{\varsigma_n} \left\{ (e^{m_{7n}t} - 1) \left(\frac{\varsigma_n^2 K^2 m_{9n}}{m_{7n}(\varsigma_n^2 + K^2)} + \frac{A_0 m_{9n}}{m_{7n}} \right) \right. \\ &+ m_{9n} A_1 e^{m_{7n}t} * \cos \omega t + m_{10n} A_1 e^{m_{8n}t} * \\ &\left. \cos \omega t + (e^{m_{8n}t} - 1) \left(\frac{\varsigma_n^2 K^2 m_{10n}}{m_{8n}(\varsigma_n^2 + K^2)} + \frac{A_0 m_{10n}}{m_{8n}} \right) \right\}. \end{aligned} \tag{31}$$

2.4.1 Fluid velocity

Bio-fluid flow is obtained by taking the inverse Hankel transform of Eq. (32)

$$u(r, t) = 2 \sum_{n=1}^{\infty} \frac{J_0(r \zeta_n)}{\zeta_n J_1^2(\zeta_n)} \times u_H(\zeta_n, t) \tag{32}$$

$$u(r, t) = 2 \sum_{n=1}^{\infty} \frac{J_0(r \zeta_n)}{\zeta_n J_1(\zeta_n)} \left\{ (e^{m_{7n}t} - 1) \left(\frac{\zeta_n^2 K^2 m_{9n}}{m_{7n}(\zeta_n^2 + K^2)} + \frac{A_0 m_{9n}}{m_{7n}} \right) + m_{9n} A_1 e^{m_{7n}t} * \cos \omega t + m_{10n} A_1 e^{m_{8n}t} * \cos \omega t + (e^{m_{8n}t} - 1) \left(\frac{\zeta_n^2 K^2 m_{10n}}{m_{8n}(\zeta_n^2 + K^2)} + \frac{A_0 m_{10n}}{m_{8n}} \right) \right\}, \tag{33}$$

for $0 < \alpha \leq 1$.

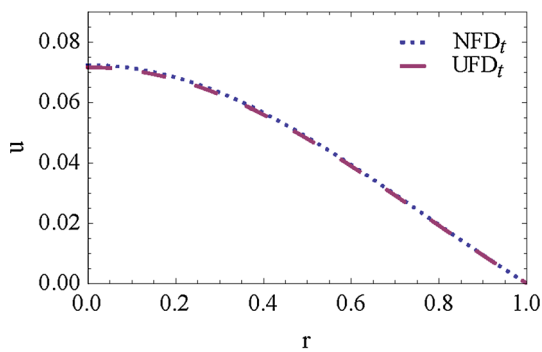
2.4.2 Magnetic particles velocity

The velocity of the magnetic particles mixed with blood is obtained from Eq. (23)

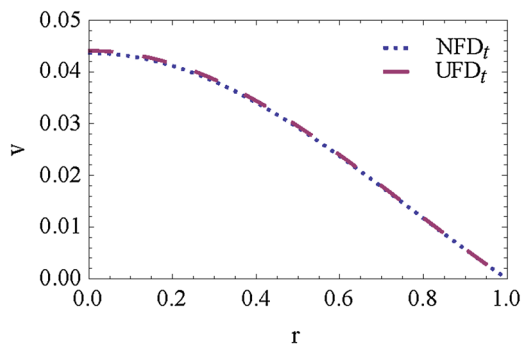
$$\bar{v}(r, s) = \frac{s + \alpha - \alpha s}{s + G s + \alpha - \alpha s} \bar{u}(r, s) \tag{34}$$

$$v(r, t) = m_{12n} (1 - m_{11n}) \{ u(r, t) * e^{-m_{12n}t} \}, \tag{35}$$

for $0 < \alpha \leq 1$.

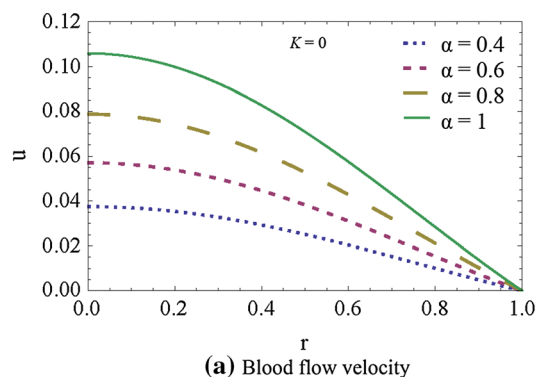


(a) Blood flow velocity

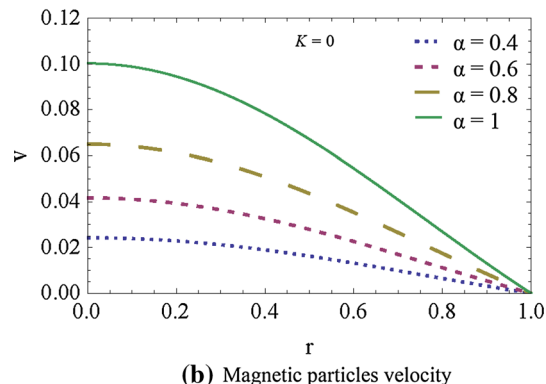


(b) Magnetic particles velocity

Fig. 2 Comparison between NFDt and UFDt at $\alpha = 1$

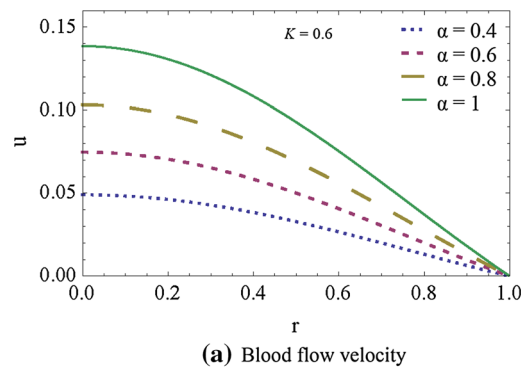


(a) Blood flow velocity

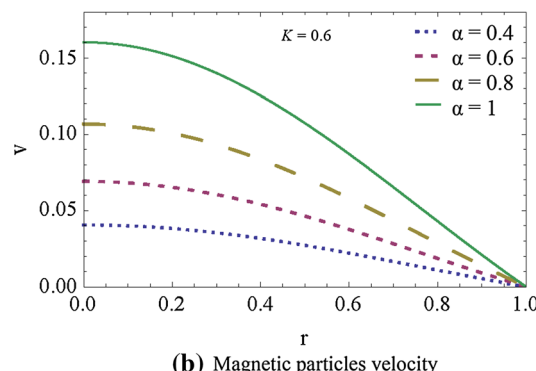


(b) Magnetic particles velocity

Fig. 3 Velocity profile for $K = 0$ and at different fractional parameters against r



(a) Blood flow velocity



(b) Magnetic particles velocity

Fig. 4 Velocity profile for $K = 0.6$ and at different fractional parameters against r

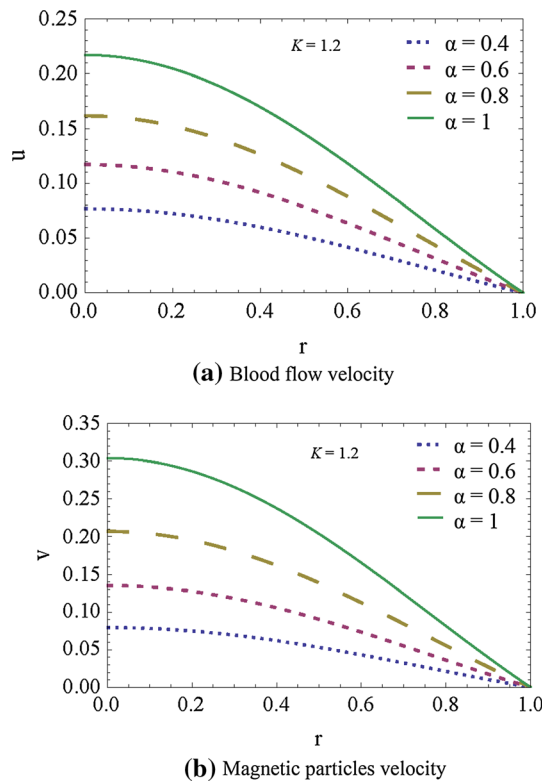


Fig. 5 Velocity profile for $K = 1.2$ and at different fractional parameters against r

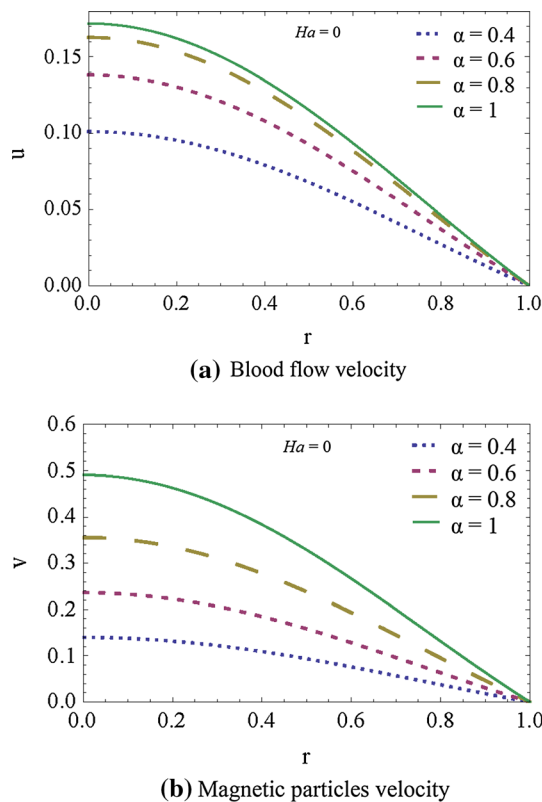


Fig. 6 Velocity profile for $Ha = 0$ and at different fractional parameters against r

In Eqs. (33) and (35) $f * g$ represents convolution product of f and g . The parameters introduced in Eq. (12) are as follows

$$m_{11n} = \frac{1 - \alpha}{G - \alpha + 1}, m_{12n} = \frac{\alpha}{G - \alpha + 1}. \tag{36}$$

Convolution product between f and g can be calculated as

$$(f * g)(t) = \int_0^t f(\tau)(t - \tau)d\tau. \tag{37}$$

3 Numerical results and discussion

Our goal was to obtain the blood flow stream parameters from the new definition of Caputo–Fabrizio fractional derivative without singular kernel solved by using both Laplace and finite Hankel transforms. A few numerical modifications were performed using the Mathematica programming. The obtained mathematical forms of $u(r, t)$ and $v(r, t)$ as shown in Eqs. (33) and (35), respectively, were graphically plotted in Figs. 2, 3, 4, 5, 6, 7, 8, 9, 10 and 11.

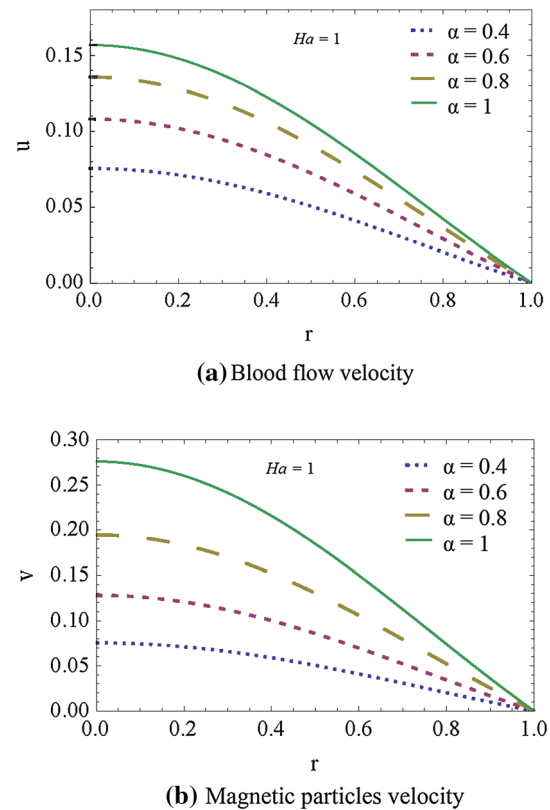
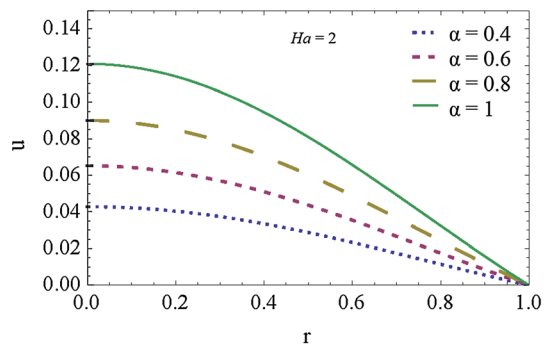
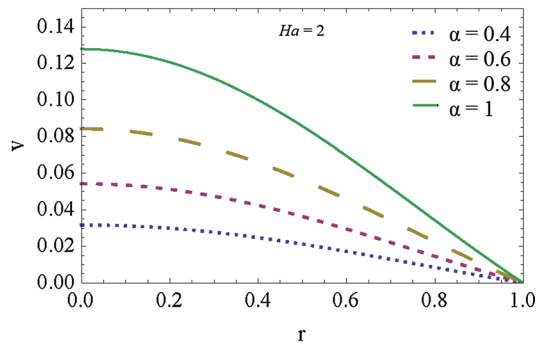


Fig. 7 Velocity profile for $Ha = 1$ and at different fractional parameters against r



(a) Blood flow velocity



(b) Magnetic particles velocity

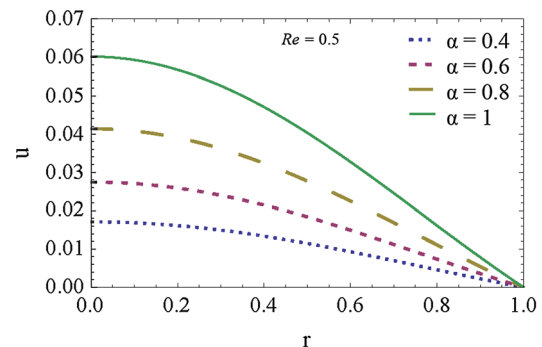
Fig. 8 Velocity profile for $Ha = 2$ and at different fractional parameters against r

It was intriguing to isolate the impact of fractional parameter on the velocities of blood and magnetic particles. The effects of electric field, magnetic field and Reynolds number were also presented. The positive root of the Bessel function “ J_0 ” was used. For all the graphical plots, the ordinary fluid model was compared with the fractional fluid model by taking $\alpha \in \{0.4, 0.6, 0.8, 1\}$. Other numerical values were $A_0 = 0.5$, $A_1 = 0.6$, $G = 0.5$, $R = 0.5$, $\omega = \pi/4$ and $t = 0.2$.

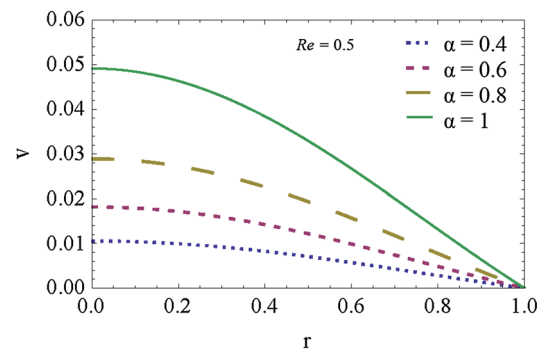
Figure 2 compares the velocity profiles for the blood flow and magnetic particles predicted using UFDt and NFDt. The velocity predicted using the local model i.e.; $\alpha = 1$ agreed well with those reported by Shah et al. (2016a) using theoretical and experimental methods.

The effects of electric field on the velocities of blood flow and magnetic particles at the core region predicted using the ordinary and fractional model were reported in Figs. 3, 4 and 5. At zero electric field, the blood flow velocity was higher than that of magnetic particles due to the drag force. Increasing external electric field would cause a more rapid development in the velocity of magnetic particles due to the collisions between charged particles. However, the fractional fluid velocity was lower than the ordinary fluid velocity.

Figures 6, 7 and 8 show the effect of external magnetic field on the velocity. Apparently, external magnetic field



(a) Blood flow velocity



(b) Magnetic particles velocity

Fig. 9 Velocity profile for $Re = 0.5$ and at different fractional parameters against r

exhibited a significant impact on the velocity profiles predicted using fractional and local models. At high values Ha , the resistive force acting on the blood flow was more intense whereby the velocity of magnetic particles dropped significantly.

The effects of Reynolds number were shown in Figs. 9, 10 and 11. Here, the velocity amplitude in the core region increased at higher Re ($Re > 1$) and the velocity of magnetic particles was higher than the blood flow velocity. At low Re ($Re < 1$), the flow behavior of blood and magnetic particles were comparable.

4 Conclusion

The flow of blood mixed with iron-rich particles (magnetic particles) was subjected to the external electro-kinetic energy and magnetic field. The flow was modeled by using the new definition of Caputo–Fabrizio fractional order derivative without singular kernel in the time fractional model. The cylindrical flow domain was considered. The governing nonlinear time fractional order differential equations were solved analytically. The velocities of blood flow and magnetic particles were obtained by taking the Laplace transform with respect to t and finite Hankel

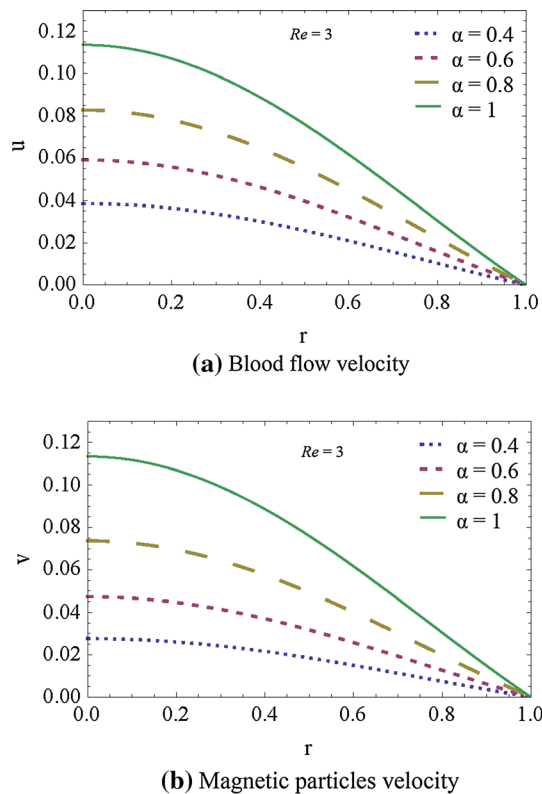


Fig. 10 Velocity profile for $Re = 3$ and at different fractional parameters against r

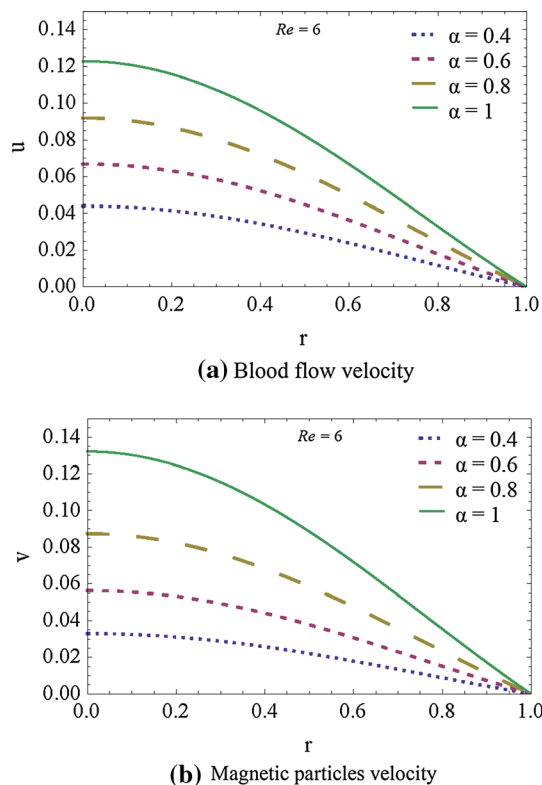


Fig. 11 Velocity profile for $Re = 6$ and at different fractional parameters against r

transform with respect to r . Graphical plots were generated using the Mathematica software. At high Reynolds number and electro kinetic energy the velocity of magnetic particles was higher than the blood flow velocity. On the other hand, at low Reynolds number and high magnetic field strength, the velocity of magnetic particles dropped tremendously.

Acknowledgements The authors would like to acknowledge the financial support received from the Universiti Tun Hussein Onn Malaysia, Grant Tier1/H070. Also, the authors extend their appreciation to the Deanship of Scientific Research at Majmaah University for funding this work under Project Number RGP-2019-16.

References

Ahmad A (2019) Flow control of non-Newtonian fluid using Riga plate: Reiner–Phillipoff and Powell–Eyring viscosity models. *J Appl Fluid Mech* 12(1):127–133

Ahmad A, Khan R (2019) A new family of unsteady boundary layer flow over a magnetized plate. *J Magnet* 24(1):75–80

Ahmed N, Shah NA, Ahmad B, Shah SIA, Ulhaq S, Rahimi-Gorji M (2018) Transient MHD convective flow of fractional nanofluid between vertical plates. *J Appl Comput Mech*. <https://doi.org/10.22055/jacm.2018.26947.1364>

Alarifi IM, Khan WS, Asmatulu R (2018) Synthesis of electrospun polyacrylonitrile-derived carbon fibers and comparison of properties with bulk form. *PLoS One* 13(8):e0201345

Alarifi IM, Abokhalil AG, Osman M, Lund LA, Ayed MB, Belmabrouk H, Tlili I (2019) MHD flow and heat transfer over vertical stretching sheet with heat sink or source effect. *Symmetry* 11(3):297

Alsagri AS, Nasir S, Gul T, Islam S, Nisar KS, Shah Z, Khan I (2019) MHD thin film flow and thermal analysis of blood with CNTs nanofluid. *Coatings* 9(3):175. <https://doi.org/10.3390/coatings9030175>

Bezi S, Souayah B, Ben-Cheikh N, Ben-Beya B (2018) Numerical simulation of entropy generation due to unsteady natural convection in a semi-annular enclosure filled with nanofluid. *Int J Heat Mass Transf* 124:841–859

Bhatti MM, Zeeshan A, Ijaz N, Beg OA, Kadir A (2017) A mathematical modeling of nonlinear thermal radiation effects on EMHD peristaltic pumping of viscoelastic dusty fluid through a porous medium duct. *Eng Sci Technol Int J* 20(3):1129–1139

Buchukuri T, Chkadua O, Natroshvili D (2016) Mixed boundary value problems of pseudo-oscillations of generalized thermo-electro-magneto elasticity theory for solids with interior cracks. *Trans A Razmadze Math Inst* 170(3):308–351

Caputo M, Fabrizio M (2015) A new definition of fractional derivative without singular kernel. *Prog Fract Differ Appl* 1(2):73–85

El-Borhamy M (2017) Numerical study of the stationary generalized viscoplastic fluid flows. *Alex Eng J* 57(3):2007–2018

Falade JA, Ukaegbu JC, Egere AC, Adesanya SO (2017) MHD oscillatory flow through a porous channel saturated with porous medium. *Alex Eng J* 56(1):147–152

Gul T, Khan MA, Noman W, Khan I, Alkanhal TA, Tlili I (2019) Fractional order forced convection carbon nanotube nanofluid flow passing over a thin needle. *Symmetry* 11(3):312. <https://doi.org/10.3390/sym11030312>

- Hussanan A, Khan I, Rahimi Gorji M, Khan WA (2019) CNTS-water-based nanofluid over a stretching sheet. *BioNanoScience*. <https://doi.org/10.1007/s12668-018-0592-6>
- Krishna ChM, Reddy GV, Souayah B, Raju CSK, Rahimi-Gorji M, Kumar Raju SS (2019) Thermal convection of MHD Blasius and Sakiadis flow with thermal convective conditions and variable properties. *Microsyst Technol*. <https://doi.org/10.1007/s00542-019-04353-y>
- Kumar DA, Varshney DCL, Singh VP (2012) Performance and analysis of blood flow with periodic body acceleration in the presence of magnetic field. *J Curr Eng Res* 2(4):25–28
- Morales-Delgado VF, Gmez-Aguilar JF, Saad KM, Khan MA, Agarwa P (2019) Analytic solution for oxygen diffusion from capillary to tissues involving external force effects: a fractional calculus approach. *Phys A* 523:48–65
- Patel A, Salehbbhai I, Banerjee J, Katiyar V, Shukla A (2012) An analytical solution of fluid flow. *Ital J Pure Appl Math* 2012:63–70
- Raju SS, Kumar KG, Rahimi-Gorji M, Khan I (2019) Darcy-Forchheimer flow and heat transfer augmentation of a viscoelastic fluid over an incessant moving needle in the presence of viscous dissipation. *Microsyst Technol*. <https://doi.org/10.1007/s00542-019-04340-3>
- Roslan R, Abdulhameed M, Hashim I, Chamkha AJ (2016) Non-sinusoidal waveform effects on heat transfer performance in pulsating pipe flow. *Alex Eng J* 55(44):3309–3319
- Rubbab Q, Mirza IA, Siddique I, Irshad S (2017) Unsteady helical flows of a size-dependent couple-stress fluid. *Adv Math Phys* 2017(9724381):1–10
- Santapuri S (2016) Thermodynamic restrictions on linear reversible and irreversible thermo-electro. *Heliyon* 2(10):1–26
- Shah NA, Vieru D, Fetecau C (2016a) Effects of the fractional order and magnetic field on the blood flow in cylindrical domains. *J Magn Magn Mater* 409:10–19
- Shah NA, Ullah S, Sajid M, Abbas Z (2016b) MHD flow and heat transfer of couple stress fluid over an oscillatory stretching sheet with heat source/sink in porous medium. *Alex Eng J* 55(2):915–924
- Sharma S, Sharma K (2014) Influence of heat sources and relaxation time on temperature distribution in tissues. *Int J Appl Mech Eng* 9(2):427–433
- Sharma S, Singh U, Katiyar V (2015) Magnetic field effect on flow parameters of blood along with magnetic particles in a cylindrical tube. *J Magn Magn Mater* 377:395–401
- Sher N, Wahid A, Tri D (2017) Nanoparticle shapes effects on unsteady physiological transport of nanofluids through a finite length non-uniform channel. *Results Phys* 7:2477–2484
- Singh J, Rathee R (2011) Analysis of non-Newtonian blood flow through stenosed vessel in porous medium under the effect of magnetic field. *Int J Phys Sci* 6(10):2497–2506
- Souayah B, Ben-Cheikh N, Ben-Beya B (2016) Numerical simulation of three-dimensional natural convection in a cubic enclosure induced by an isothermally-heated circular cylinder at different inclinations. *Int J Therm Sci* 110:325–339
- Souayah B, Ben-Cheikh N, Ben-Beya B (2017a) Effect of thermal conductivity ratio on flow features and convective heat transfer. *Part Sci Technol* 35(5):565–574
- Souayah B, Ben-Cheikh N, Ben-Beya B (2017b) Periodic behavior flow of three-dimensional natural convection in a titled obstructed cubical enclosure. *Int J Numer Methods Heat Fluid Flow* 27(9):2030–2052
- Souayah B, Reddy MG, Poornima T, Rahimi-Gorji M, Alarifi IM (2019) Comparative analysis on non-linear radiative heat transfer on MHD Casson nanofluid past a thin needle. *J Mol Liq* 284:163–174
- Tanveer S (2016) Steady blood flow through a porous medium with periodic body acceleration and magnetic field. *Comput Appl Math J* 2(1):1–5
- Tripathi Dharmendra, Bhushan Shashi, Beg O Anwar (2018) Unsteady viscous flow driven by the combined effects of peristalsis and electro-osmosis. *Alex Eng J* 57(3):1349–1359
- Usman M, Hamid M, Khan U, Tauseef S, Din M, Asad M, Wang W (2018) Differential transform method for unsteady nanofluid flow and heat transfer. *Alex Eng J* 50(3):1867–1875

Publisher's Note Springer Nature remains neutral with regard to jurisdictional claims in published maps and institutional affiliations.